OPEN

npg

Triptolide induces apoptosis in human leukemia cells through caspase-3-mediated ROCK1 activation and MLC phosphorylation

L Liu[1,3], G Li[1,3], Q Li[2], Z Jin[1], L Zhang[1], J Zhou[1], X Hu[1], T Zhou[1], J Chen[*,2] and N Gao[*,1]

The diterpene triepoxide triptolide is a major active component of *Tripterygium wilfordii* Hook F, a popular Chinese herbal medicine with the potential to treat hematologic malignancies. In this study, we investigated the roles of triptolide in apoptosis and cell signaling events in human leukemia cell lines and primary human leukemia blasts. Triptolide selectively induced caspase-dependent cell death that was accompanied by the loss of mitochondrial membrane potential, cytochrome *c* release, and Bax translocation from the cytosol to the mitochondria. Furthermore, we found that triptolide dramatically induced ROCK1 cleavage/activation and MLC and MYPT phosphorylation. ROCK1 was cleaved and activated by caspase-3, rather than RhoA. Inhibiting MLC phosphorylation by ML-7 significantly attenuated triptolide-mediated apoptosis, caspase activation, and cytochrome *c* release. In addition, ROCK1 inhibition also abrogated MLC and MYPT phosphorylation. Our *in vivo* study showed that both ROCK1 activation and MLC phosphorylation were associated with the tumor growth inhibition caused by triptolide in mouse leukemia xenograft models. Collectively, these findings suggest that triptolide-mediated ROCK1 activation and MLC phosphorylation may be a novel therapeutic strategy for treating hematological malignancies.

Rho GTPase family proteins, including Rho, Rac1, and Cdc42, control a wide variety of cellular processes such as cell adhesion, motility, proliferation, differentiation, and apoptosis.[1] Rho-associated coiled-coil-containing protein kinase (ROCK) is one of the best characterized Rho effectors.[2] ROCK is a serine/threonine protein kinase that is activated via interactions with Rho GTPases.[3] ROCK activity is responsible for stabilizing actin microfilaments as well as promoting cellular contraction and cell substratum contact.[4]

The ROCK family comprises two members: ROCK1 and ROCK2.[5] Both ROCK1 and ROCK2 phosphorylate a variety of protein substrates at serine or threonine residues, including myosin light chain (MLC)[6] and the myosin binding subunit of MLC phosphatase (MYPT).[7] ROCK can increase MLC phosphorylation directly by acting on MLC or indirectly by inactivating MYPT.[8] Increasing MLC phosphorylation and inactivating MYPT play important physiological roles in regulating the actin cytoskeleton.[9]

ROCK activity can be regulated by several proteins, such as RhoA or caspase-3. The Rho-binding domain of ROCKs interacts with the active GTP-bound form of RhoA, thereby disrupting the interaction between RhoA and the inhibitory carboxyl-terminal region of ROCK.[2] ROCK can also be constitutively activated by proteolytic cleavage of this inhibitory carboxyl-terminal domain. ROCK1 is cleaved by caspase-3 during apoptosis.[10,11] In apoptotic cells, ROCK1 is not cleaved in caspase-3-deficient MCF-7 breast carcinoma cells unless procaspase-3 expression is restored.[11] In addition, caspase-3-mediated ROCK1 cleavage can be inhibited by caspase inhibitors in a variety of apoptotic cells.[10–14]

Triptolide, a diterpene triepoxide (Figure 1a), is a major active component of *Tripterygium wilfordii* Hook F (TWHF) extracts. Triptolide has multiple pharmacological activities, including anti-inflammatory, immune modulation, and anti-tumor activities.[15] The antitumor effects of triptolide have recently attracted considerable attention. Triptolide inhibits proliferation and induces apoptosis in various cancer cell lines *in vitro* and inhibits tumor growth and metastases *in vivo*[16] through multiple mechanisms, including: downregulating the antiapoptotic proteins XIAP, Mcl-1, and Bcr-Abl;[17–19] upregulating p53, p21, and Bcl2-associated X protein (Bax);[20–22] suppressing HSP70;[23] and downregulating MDR1.[24]

[1]Department of Pharmacognosy, College of Pharmacy, 3rd Military Medical University, Chongqing, China and [2]Department of Hematology, Southwest Hospital, 3rd Military Medical University, Chongqing, China
*Corresponding authors: N Gao, Department of Pharmacognosy, College of Pharmacy, 3rd Military Medical University, Chongqing 400038, China. Tel: +86 23 68753736; Fax: +86 23 68753046; E-mail: gaoning59@gmail.com
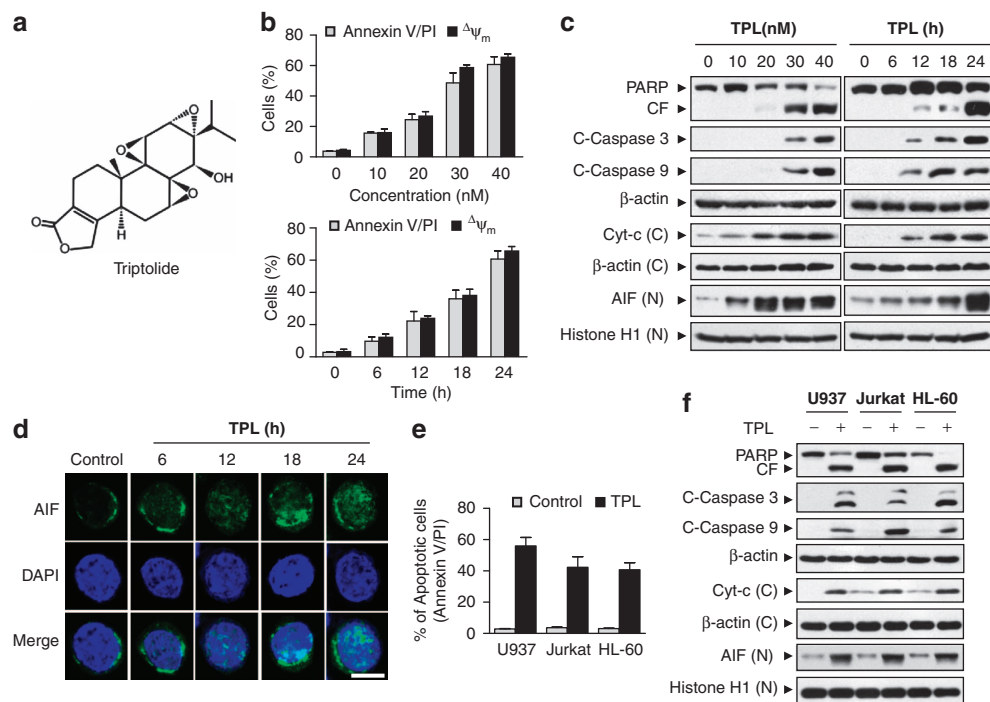or J Chen, Department of Hematology, Southwest Hospital, 3rd Military Medical University, Chongqing 400038, China. Tel: +086 13983766908; Fax: +86 23 68765196; E-mail: chenjpxn@163.com
[3]These authors contributed equally to this work.

Figure 1 Triptolide induced apoptosis and mitochondrial injury in multiple leukemia cell lines. (**a**) The chemical structure of triptolide, $C_{20}H_{24}O_6$, molecular weight: 360.4. (**b** and **c**) U937 cells were treated with various triptolide (TPL) concentrations for 24 h or with 40 nM triptolide for different lengths. The percentage of apoptotic cells was determined by FACS analysis using Annexin V/PI staining. Mitochondrial membrane potentials ($\Delta\Psi m$) were detected by rhodamine-123 staining and flow cytometry. Values represent the mean $\pm$ S.D. for five separate experiments. Total protein lysates, nuclear extracts, and cytosolic fractions were analyzed by immunoblotting using the indicated antibodies. (**d**) After triptolide treatment, cells were collected and stained with anti-AIF (green) and 4′,6-diamidino-2-phenylindole (DAPI; blue) to identify cellular nuclei. Fluorescence was visualized by a laser confocal scanning microscope. Scale bar represents 10 μm. These data are representative of three independent experiments. (**e** and **f**) U937, Jurkat, and HL-60 cells were treated with or without 40 nM triptolide for 24 h, after which apoptosis was determined by FACS analysis using Annexin V/PI staining. Total protein lysates, nuclear extracts, and cytosolic fractions were analyzed by immunoblotting using the indicated antibodies. CF, cleavage fragment; C, cytosolic fractions; N, nuclear extracts

Several signaling pathways have also been reportedly involved in triptolide-mediated apoptosis. For instance, triptolide can induce apoptosis by inhibiting NF-κB and activating MAPKs.[25] In cervical cancer cells, triptolide inactivates Akt and induces caspase-dependent death via mitochondrial apoptosis,[26] and in acute myeloid leukemia (AML) cells, triptolide induces apoptosis by inhibiting JAK/STAT signaling.[27] The molecular mechanisms of triptolide-induced apoptosis in human leukemia cells have not been fully explored.

In the present study, we examined the effects of triptolide on apoptosis in various leukemia cell lines and primary human leukemia blasts. For the first time, we show that triptolide selectively induces apoptosis in human leukemia cells through the ROCK1/MLC signaling pathway and that caspase-3-mediated ROCK1 activation is involved in this process. Our *in vivo* study also showed that ROCK1 activation and MLC phosphorylation are associated with the triptolide-mediated inhibition of U937 xenograft growth in nude mice. Because triptolide is currently being evaluated in clinical trials for treating cancer, especially human leukemia,[28] understanding its antileukemic activity may have potential clinical implications.

Results

Triptolide selectively induced apoptosis and mitochondrial injury in multiple leukemia cell lines and primary human leukemia blasts. The dose-dependent effects of

triptolide on apoptosis in U937 cells were determined using flow cytometry analysis. Exposing U937 cells to 10 nM triptolide resulted in a moderate increase in apoptosis, and 20, 30, and 40 nM triptolide exacerbated this effect (Figure 1b). A time-course analysis showed that cells exposed to 40 nM triptolide experienced a slight increase in apoptosis as early as at 6 h of exposure; this increase in apoptosis became even more apparent at 12, 18, and 24 h of drug exposure (Figure 1b).

The outer mitochondrial membrane becomes permeable during mitochondrial apoptosis, a process that is necessary for cytochrome *c* release and caspase acitvation.[29] We investigated mitochondrial alterations as well as caspase activation in response to triptolide treatment. Exposing U937 cells to triptolide resulted in a pronounced loss of mitochondrial membrane potential ($\Delta\psi_m$) in both dose- and time-dependent manners (Figure 1b). Consistent with these findings, the same triptolide concentrations and exposure lengths resulted in significant caspase-3, caspase-9, and poly-ADP-ribose polymerase (PARP) cleavage, cytochrome *c* release, and nuclear apoptosis-inducing factor (AIF) accumulation (Figure 1c). The time-dependent nuclear AIF accumulation was also observed by immunofluorescence in cells exposed to triptolide (Figure 1d).

To determine whether triptolide-induced apoptosis was specific for U937 cells, parallel studies were performed using other human leukemia cell types, including Jurkat

T-lymphoblasts and HL-60 promyelocytic leukemia cells. These cell lines exhibited apoptotic effects similar to those in U937 cells (Figure 1e). In addition, Jurkat and HL-60 cells had comparable degrees of caspase-3 and caspase-9 activation, PARP cleavage, cytochrome *c* release, and nuclear AIF accumulation (Figure 1f).

Primary mononuclear cells were also isolated from 44 leukemia patients (29 with AML, 2 with acute lymphocytic leukemia, 11 with chronic myelogenous leukemia, and 2 with chronic lymphocytic leukemia) to determine whether triptolide could also trigger apoptosis in primary human leukemia cells. Cells were treated with or without 40 nM triptolide for 24 and 36 h, and apoptosis levels were measured by flow cytometry. The characteristics of the leukemia patient samples are summarized in Supplementary Table S1. Exposure to 40 nM triptolide for 24 h resulted in a significant increase in apoptosis in primary leukemic blasts (mean increase of 36.37% for

triptolide treatment *versus* 13.14% for control cells, $P < 0.0001$, $n = 44$). Exposing cells for 36 h exacerbated this increase in apoptosis (mean increase of 54.53% for triptolide treatment *versus* 13.14% for control cells, $P < 0.0001$, $n = 44$; Figure 2a). Treating leukemia blasts from four AML patients with triptolide also resulted in caspase-3, caspase-9, and PARP cleavage, and cytochrome *c* release (Figure 2b).

The same triptolide concentrations and exposure lengths had minimal lethality in normal CD34$^+$ cells isolated from the bone marrow of six healthy donors (Figure 2c). The characteristics of the healthy donors are summarized in Supplementary Table S1. Triptolide treatment also had no apparent effect on caspase-3, caspase-9, and PARP cleavage in normal CD34$^+$ cells (Figure 2d).

Bax translocation was induced by triptolide-mediated apoptosis. Bax is an important proapoptotic factor that is
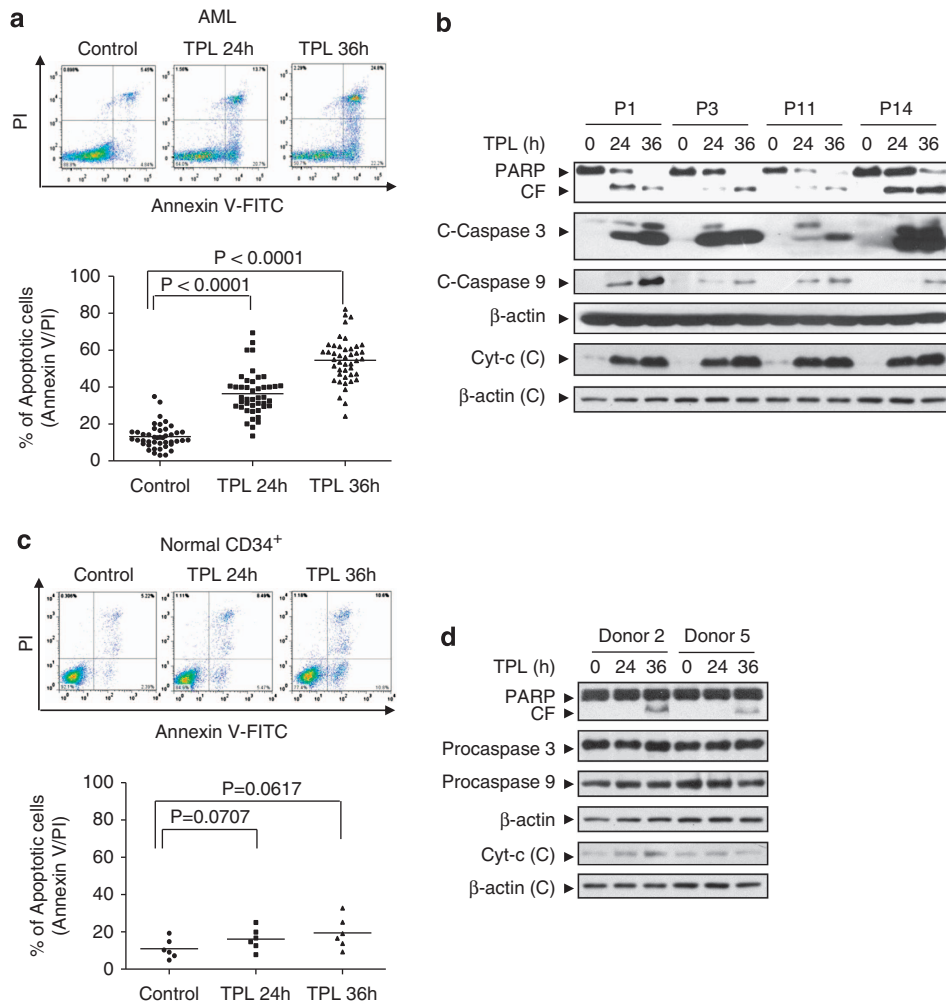
Figure 2 Triptolide induced apoptosis in primary human leukemia blasts but not in normal CD34$^+$ cells. (a) Primary leukemia blasts from 44 patients were treated with 40 nM triptolide for 24 or 36 h, after which apoptosis was determined by FACS analysis using Annexin V/PI staining. Upper panel: representative FACS images. Lower panel: numbers indicate the percentage of apoptotic cells; each symbol represents results from individual patients. (b) Total protein lysates and cytosolic fractions of the samples from four AML patients were then obtained and analyzed by immunoblotting using the indicated antibodies. (c) Normal CD34$^+$ cells were isolated from 6 normal bone marrow samples and exposed to 40 nM triptolide for 24 or 36 h. The percentage of apoptotic cells was determined by FACS analysis using Annexin V/PI staining. (d) Two normal donors were treated with 40 nM triptolide for 24 or 36 h. Total protein lysates and cytosolic fractions of these samples were then obtained and analyzed by immunoblotting using the indicated antibodies

involved in mitochondrial apoptosis. Following a death signal, Bax is translocated from the cytosol to the outer mitochondrial membrane where it promotes the release of different apoptogenic factors, such as cytochrome *c*, via membrane permeabilization.[30] We examined the intracellular localization of Bax in mitochondrial and cytosolic fractions using immunoblots. Bax was predominantly found in the cytosolic fraction of untreated control cells (Figure 3a). Triptolide redistributed Bax from the cytosolic to mitochondrial compartment.

We also investigated the sub-cellular localization of Bax during triptolide-induced apoptosis using immunofluorescence microscopy. In untreated cells, Bax was mostly distributed in the cytosol; however, upon triptolide treatment, there was a clear shift in Bax localization from the cytosol to the mitochondria (Figure 3b). This Bax translocation was also observed in Jurkat and HL-60 cells treated with triptolide (Figure 3c). These findings suggest that Bax translocation may contribute to apoptosis in cells that are exposed to triptolide.

ROCK1 activation and MLC and MYPT phosphorylation contributed to triptolide-mediated apoptosis. Studies have shown that ROCK1 activity may be necessary for cytoskeletal reorganization and membrane blebbing during apoptosis.[10] We examined the effects of triptolide on ROCK1 expression. Cells treated with 20 nM triptolide for 24 h experienced a modest decrease in ROCK1 expression and increased ROCK1 cleavage. These events became even more apparent at 30 and 40 nM triptolide (Figure 4a). A time-course study of cells exposed to 40 nM triptolide revealed a moderate increase in ROCK1 cleavage and activation after 12 h of drug exposure; these events became more obvious after 18 and 24 h of drug exposure (Figure 4a).

As ROCK1 is a major target of RhoA,[31] we also evaluated the effect of triptolide on RhoA activation. RhoA activation was measured in U937 cells treated with triptolide using a GST-RBD (glutathione *S*-transferase-RhoA binding domain of Rhotekin) pull-down assay. Unfortunately, triptolide treatment did not affect RhoA activation (RhoA-GTP) and total RhoA levels (Figure 4a).

ROCK1 has also been recently shown to regulate MLC phosphorylation that is necessary for forming dynamic membrane blebs during apoptosis.[11] Therefore, we evaluated phosphorylated MLC levels during triptolide-induced apoptosis. Cells treated with 20 nM triptolide for 24 h had slightly

elevated levels of phospho-MLC that increased in cells treated with 30 and 40 nM triptolide (Figure 4a). A time-course analysis of cells exposed to 40 nM triptolide found that phospho-MLC levels slightly increased after 12 h of drug exposure; this increase became more apparent after 18 and 24 h of drug exposure (Figure 4a). In contrast, triptolide treatment had no effect on total MLC levels (Figure 4a).

Studies have also reported that the ROCKs also phosphorylate MYPT.[32] MYPT phosphorylation blocks MLC dephosphorylation, leading to MLC activation.[33] We determined the effects of triptolide on MYPT phosphorylation. Exposing U937 cells to triptolide markedly increased phospho-MYPT levels in both dose- and time-dependent manners (Figure 4a). In contrast, triptolide treatment had no effect on the expression of total MYPT (Figure 4a).

Triptolide-mediated ROCK1 activation and MLC and MYPT phosphorylation were also observed in other leukemia cell lines, including Jurkat and HL-60 cells (Figure 4b) and primary AML blasts (Figure 4c). However, these events were not observed in normal CD34^{+} bone marrow cells (Figure 4d). Taken together, these findings suggest that the ROCK1/MLC pathway may play an important role in triptolide-induced apoptosis in human leukemia cells.

Caspase-3, rather than RhoA, activated ROCK1 during triptolide-induced apoptosis. ROCK1 is a prominent caspase-3 substrate that is cleaved and activated during apoptosis.[10,14] We examined the effects of caspase inhibitors (z-VAD-fmk or z-DEVD-fmk) on ROCK1 cleavage and MLC phosphorylation during triptolide-induced apoptosis. Pretreatment with z-VAD-fmk or z-DEVD-fmk significantly abrogated the triptolide-induced increase in apoptosis in both U937 cells and primary AML blasts (Figure 5a). Cotreatment of triptolide with z-VAD-fmk or z-DEVD-fmk also blocked the previously observed caspase-3 and PARP cleavage (Figure 5b). Interestingly, inhibiting caspase activity by z-VAD-fmk or z-DEVD-fmk also significantly blocked the ROCK1 activation and MLC phosphorylation mediated by triptolide (Figure 5c). These findings suggest that caspase-3 is responsible for activating ROCK1 and, therefore, phosphorylating MLC during triptolide-induced apoptosis.

As the kinase activity of ROCK1 is enhanced during apoptosis after ROCK1 binds RhoA,[34] we also investigated the effects of C3 exoenzyme, a RhoA inhibitor, on ROCK1 cleavage and activation during triptolide-induced apoptosis. Pretreatment of U937 cells and AML blasts with C3 did not
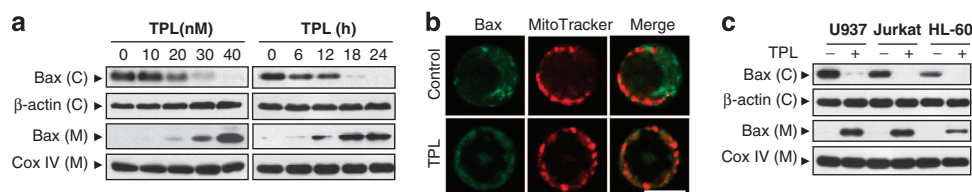
Figure 3 Triptolide induced Bax translocation in multiple leukemia cell lines. (**a**) U937 cells were treated with various triptolide concentrations for 24 h or with 40 nM triptolide for different lengths, after which cytosolic and mitochondrial fractions were isolated and subjected to immunoblot analysis by using an anti-Bax antibody. (**b**) U937 cells were treated with or without 40 nM triptolide for 24 h. Cells were collected and stained with anti-Bax (green) and MitoTracker (red) to identify mitochondria. Fluorescence was visualized by a laser confocal scanning microscope. Scale bar represents 10 μm. These data are representative of three independent experiments. (**c**) U937, Jurkat, and HL-60 cells were treated with or without 40 nM triptolide for 24 h, after which cytosolic and mitochondrial fractions were isolated and subjected to immunoblot analysis by using an anti-Bax antibody
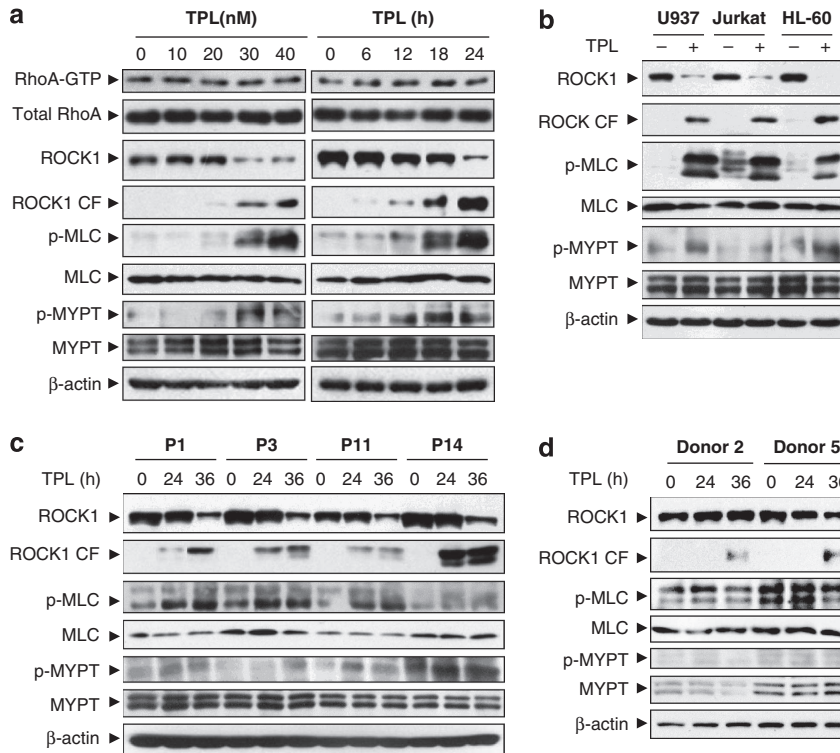
Figure 4 Triptolide induced ROCK1 activation and MLC and MYPT phosphorylation. (**a**) U937 cells were treated with various triptolide concentrations for 24 h or with 40 nM triptolide for different lengths. Total protein lysates were analyzed by immunoblotting using the indicated antibodies. RhoA-GTP was evaluated using a Rhotekin RBD-GST pull-down. (**b**) U937, Jurkat, and HL-60 cells were treated with or without 40 nM triptolide for 24 h. Total protein lysates were analyzed by immunoblotting using the indicated antibodies. Samples from four AML patients (**c**) and two normal donors (**d**) were treated with 40 nM triptolide for 24 or 36 h. The total protein lysates of these samples were obtained and analyzed by immunoblotting using the indicated antibodies

diminish the triptolide-mediated increase in apoptosis, PARP cleavage, and caspase activation (Figures 5d and e). In addition, pretreatment with C3 did not abrogate the ROCK1 activation and MLC and MYPT phosphorylation induced by triptolide (Figure 5f). Taken together, these findings indicate that caspase-3, rather than RhoA, activates ROCK1 in triptolide-induced apoptosis.

ROCK1 activation and MLC phosphorylation may have important functional roles in triptolide-mediated apoptosis. ML-7, a specific MLC inhibitor, was used to further characterize the role of MLC in triptolide-mediated apoptosis. Pretreating both U937 cells and primary AML blasts with ML-7 (20 μM) dramatically attenuated triptolide-mediated apoptosis (Figure 6a). Consistently, co-administering ML-7 with triptolide also reduced the PARP cleavage, caspase activation, and cytochrome *c* release induced by triptolide (Figure 6b). Western blots also showed that pretreatment with ML-7 inhibited the triptolide-mediated MLC phosphorylation (Figure 6c).

ROCK1 regulates MLC phosphorylation, and apoptotic cells exhibit gradual increases in phosphorylated MLC levels concomitant with ROCK1 cleavage.[11] We investigated whether modulating ROCK1 phosphorylation of MLC affected triptolide-induced apoptosis. Pretreating U937 and AML cells with Y27632, a ROCK1 inhibitor, dramatically prevented triptolide-mediated apoptosis (Figure 7a). Consistent with these findings, pretreating U937 cells and AML blasts with

Y27632 also attenuated PARP cleavage, caspase activation, and cytochrome *c* release induced by triptolide (Figure 7b). Furthermore, pretreating with Y27632 dramatically abrogated the triptolide-induced ROCK1 activation and MLC and MYPT phosphorylation (Figure 7c).

Next, we knocked down ROCK1 expression in U937 cells using a ROCK1-specific short interfering RNA (siRNA). Knocking down ROCK1 expression significantly abrogated triptolide-mediated apoptosis and diminished triptolide-induced PARP cleavage, caspase activation, and cytochrome *c* release (Figures 7d and e). Western blots showed that U937 cells transfected with ROCK1 siRNA had reduced total ROCK1 and cleaved ROCK1 expression. Knocking down ROCK1 also reduced the triptolide-induced MLC and MYPT phosphorylation (Figure 7f). Taken together, these findings suggest that the ROCK1/MLC signaling pathway has an important functional role in triptolide-mediated apoptosis.

Triptolide suppressed tumor growth, induced apoptosis, and activated ROCK1/MLC signaling in a U937 xenograft model. To determine whether triptolide exhibits antileukemic activity *in vivo*, nude mice were inoculated with U937 xenografts. Decreased tumor growth was apparent 15 days after initiating triptolide treatment (0.15 mg/kg; $P < 0.05$ *versus* vehicle control). This suppressed tumor growth became more apparent after 20 days ($P < 0.01$ *versus* vehicle control) and 25–40 days ($P < 0.0001$ *versus* vehicle control; Figure 8a). In contrast, no statistically
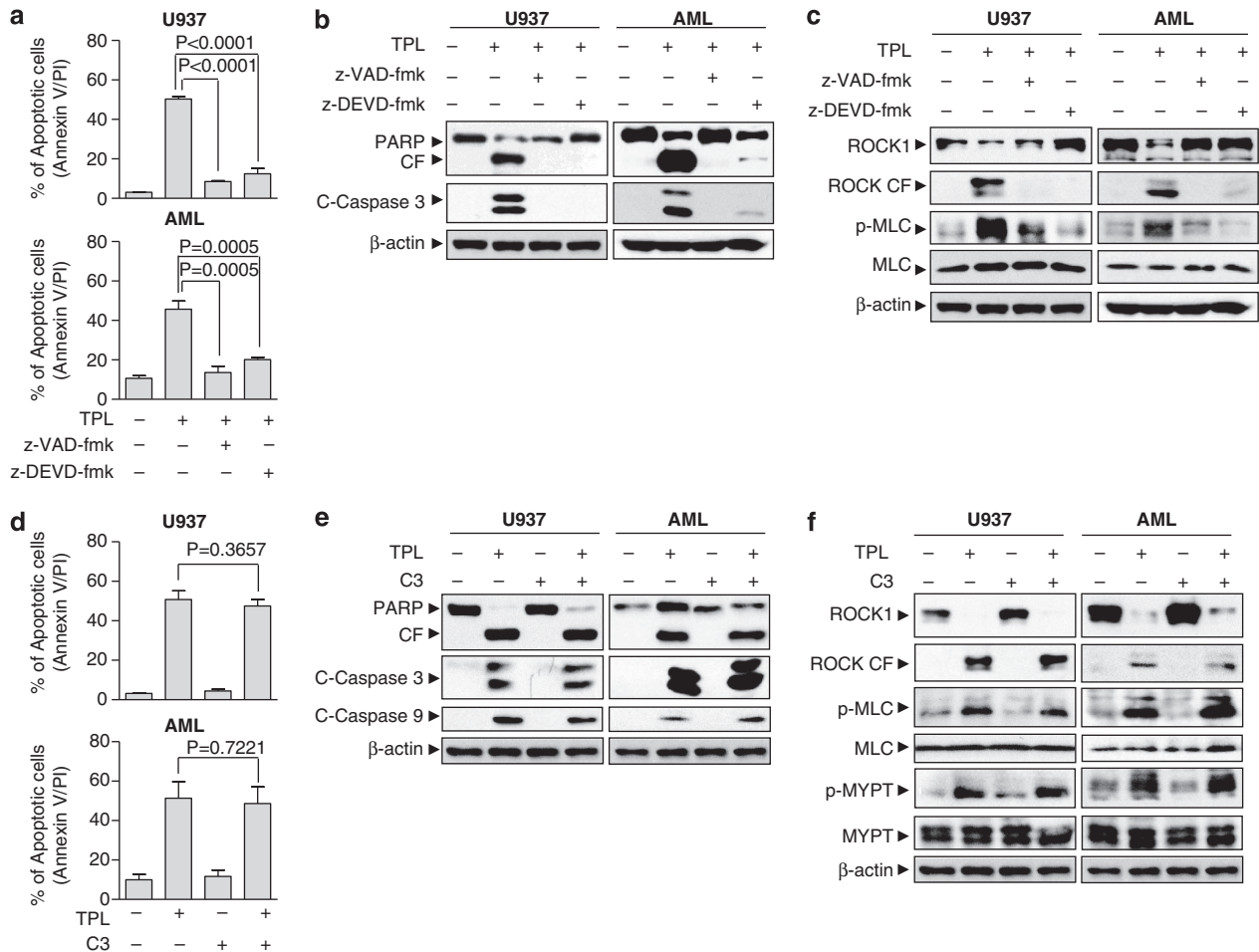
Figure 5 Caspase-3, rather than RhoA, activated ROCK1 during triptolide-induced apoptosis. Caspase inhibitors (z-VAD-fmk or z-DEVD-fmk) and a Rho inhibitor (C3 exoenzyme) were used to explore the mechanism behind ROCK1 activation. The percentage of apoptotic cells was determined by FACS analysis using Annexin V/PI staining. Error bars represent the mean ± S.D. ($n = 5$). Total protein lysates were analyzed by immunoblotting using the indicated antibodies. Results are representative of three independent experiments. (**a–c**) U937 cells and blasts from one AML patient were pretreated with 20 μM z-VAD-fmk or z-DEVD-fmk for 2 h followed by treatment with or without 40 nM triptolide for 24 h. (**d–f**) U937 cells and blasts from one AML patient were transfected with 5 μg C3 (premixed with FuGENE 6 Reagent in RPMI-1640 medium). After 5 h of incubation, cells were treated with or without 40 nM triptolide for 24 h

significant changes in body weight were noted when comparing triptolide-treated and control mice (Figure 8b). Moreover, mice in the triptolide group did not exhibit any signs of toxicity such as agitation, impaired movement or posture, indigestion or diarrhea, and areas of redness or swelling. These findings indicate that triptolide administration significantly inhibited U937 xenograft growth without causing any side effects and/or toxicity in these mice.

Tumor samples were excised, sectioned, and analyzed by hematoxylin and eosin (H&E) staining and TdT-mediated dUTP nick-end labeling (TUNEL) assays to evaluate morphological changes and apoptosis in U937 cells in vivo. Tumors from control mice had typical histologic appearances whereas that of mice treated with triptolide had a marked decrease in cancer cells and signs of necrosis, inflammatory cell infiltration, and fibrosis (Figure 8c, top panels). Administering triptolide also significantly induced apoptosis in tumor cells, as measured by TUNEL positivity (Figure 8c, second panel). Immunohistochemistry analysis further revealed that triptolide-treated mice had increased immunoreactivity for

cleaved caspase-3, another indicator of apoptosis (Figure 8c, third panel).

To further evaluate whether ROCK1/MLC signaling pathway could be involved in antileukemic activity mediated by triptolide in vivo, western blot and immunohistochemistry analyses were employed. Treating mice with triptolide resulted in dramatic increase in the levels of phospho-MLC (Figure 8c, bottom panels). Furthermore, treatment with triptolide resulted in a clear increase in cleavage/activation of ROCK1 (Figure 8d). Taken together, these findings indicate that triptolide significantly inhibited the growth of U937 xenografts without causing any side effects and that this effect was also associated with ROCK1 activation and MLC phosphorylation.

Discussion

In the present study, we demonstrated that triptolide selectively induced mitochondrial injury and apoptosis in multiple human leukemia cell lines and primary human
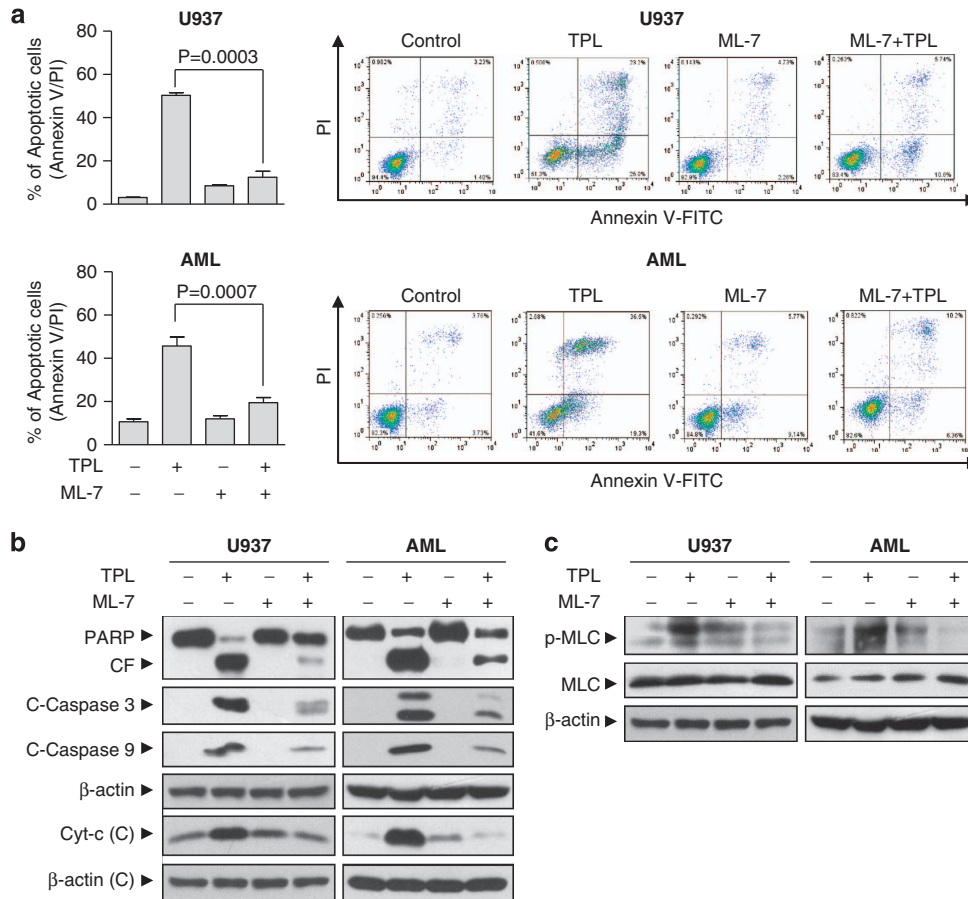
Figure 6 Inhibiting MLC phosphorylation significantly decreased triptolide-induced apoptosis. U937 cells and blasts from one AML patient were pretreated with 20 μM ML-7, a MLC kinase inhibitor, for 2 h followed by treatment with or without 40 nM triptolide for 24 h. (**a**) The percentage of apoptotic cells was determined by FACS analysis using Annexin V/PI staining. Error bars represent the mean $\pm$ S.D. ($n = 5$). (**b** and **c**) Total protein lysates and cytosolic fractions were analyzed by immunoblotting using the indicated antibodies. Results were representative of three independent experiments

leukemia blasts *in vitro* at low nM concentrations (Figures 1 and 2) and also inhibited the growth of U937 xenografts at low dosage (0.15 mg/kg/day, i.p.; Figure 8). Yang *et al.*[35] reported that the antitumor effect of triptolide (at nM concentrations) was comparable or even superior to that of conventional antitumor drugs (at μM concentrations) such as adriamycin, mitomycin, and cisplatin. Similarly, in the mouse model system, triptolide was more potent than adriamycin, mitomycin, or cisplatin in inhibiting the growth of tumor xenografts.[35] Our and other results suggest that triptolide has very attractive features as an antitumor agent with regard to its high potency. Because triptolide selectively kills leukemia cells and inhibits the tumor growth of U937 xenografts without apparent toxicity, triptolide could be developed into a new antitumor agent for treating leukemia.

Mitochondria are cellular organelles that regulate commitment to and execution of apoptosis.[36] Mitochondrial outer membrane permeabilization (MOMP) allows cell death factors such as cytochrome *c* to be released into the cytoplasm, thus inducing caspase activation and apoptosis.[37] MOMP is mainly controlled by the Bcl-2 family of proteins that consists of both proapoptotic and antiapoptotic members.[38] Numerous studies showed that triptolide-induced apoptosis depends on mitochondrial-mediated pathway in various types of cancer

cells. Triptolide induces apoptosis in cervical cancer cells that was accompanied by loss of mitochondrial membrane potential and cleavage/activation of caspase-3, -9, and PARP.[26] Downregulation of Mcl-1 may contribute to mitochondrial cell death mediated by triptolide. Triptolide induces apoptosis in human adrenal cancer NCI-H295 cells through a mitochondrial-dependent pathway (i.e., the loss of mitochondrial membrane potential, cytochrome *c* and Apaf-1 release, and activation of caspase-3 and caspase-9).[39] It has also been shown that triptolide induces mitochondrial-dependent apoptosis in multiple human leukemia cell lines and primary leukemia blasts through downregulation of XIAP and Mcl-1.[17,40] Consistent with these reports, our results showed that triptolide-induced apoptosis in human leukemia cells is accompanied by the loss of mitochondrial membrane potential (Figure 1b) and release of cytochrome *c* into the cytoplasm (Figure 1c). Bax translocation from the cytosol to the mitochondria may be involved in triptolide-mediated mitochondrial damage and apoptosis. Our findings indicate that triptolide-mediated apoptosis in human leukemia cells proceeds through the mitochondrial pathway.

In this study, we also provided evidence that the ROCK1/ MLC signaling pathway plays an essential role in this triptolide-mediated apoptosis. ROCK1 is one of two ROCK
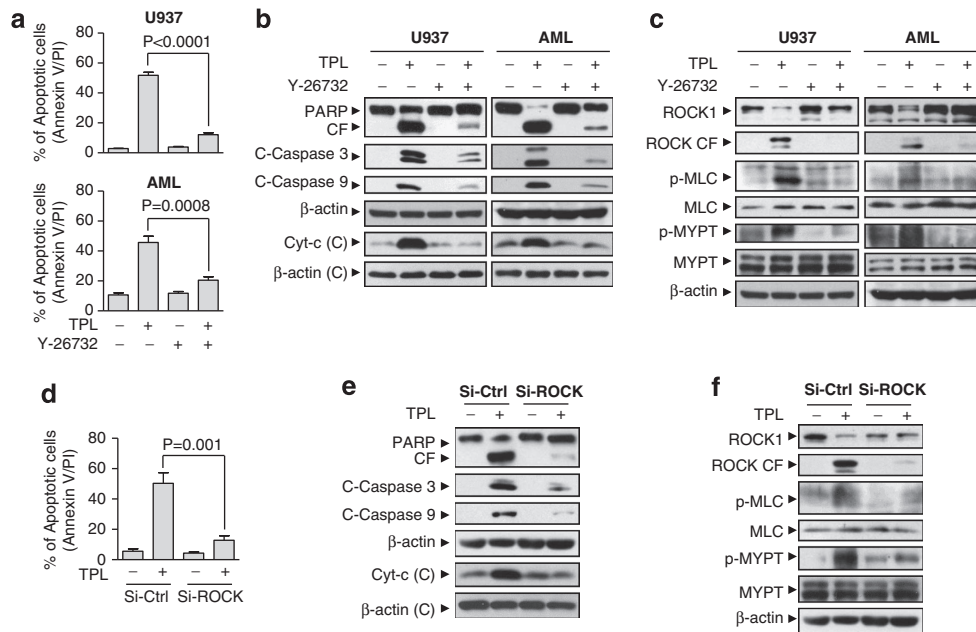
Figure 7 Inhibiting ROCK1 activation attenuated triptolide-induced apoptosis. (**a**) U937 cells and blasts from one AML patient were pretreated with 20 μM Y-27632, a ROCK1 inhibitor, for 2 h followed by treatment with 40 nM triptolide for 24 h. The percentage of apoptotic cells was determined by FACS analysis using Annexin V/PI staining. Error bars represent the mean $\pm$ S.D. ($n = 5$). (**b** and **c**) Total protein lysates and cytosolic fractions were analyzed by immunoblotting using the indicated antibodies. Results are representative of three independent experiments. (**d**) U937 cells were stably transfected with lentivirus containing ROCK1-specific siRNA (si-ROCK1) or a scrambled control siRNA. Cells were treated with or without 40 nM triptolide for 24 h, and apoptosis was measured by FACS analysis using Annexin V/PI staining. Error bars represent the mean $\pm$ S.D. ($n = 5$). (**e** and **f**) Total protein lysates and cytosolic fractions were analyzed by immunoblotting using the indicated antibodies. Results are representative of three independent experiments

isoforms (ROCK1 and ROCK2). ROCK is a known effector of Rho GTPases that are involved in various cellular processes such as apoptosis.[31] A number of studies have revealed that ROCK is frequently deregulated in many human cancers. ROCK1 mutations contribute to cancer progression and have been identified in human tumors with elevated kinase activities.[41]

ROCK1 activity can be regulated by several distinct mechanisms, including RhoA and caspase-3 activation. ROCK1 is activated by RhoA-GTP via a conformational change that shifts the inhibitory carboxyl-terminal domain of ROCK1 away from its active kinase site.[2] The RhoA/ROCK1 pathway is activated by numerous extracellular stimuli. For example, ethanol induces RhoA-mediated ROCK1 activation,[42] and lipid mediators, such as arachidonic acid (AA) and sphingosylphosphorylcholine (SPC), can also interact with the inhibitory ROCK carboxyl-terminal domain to stimulate ROCK activity independent of RhoA. At the cellular level, AA or SPC/ROCK pathways mainly increase calcium sensitivity in smooth muscle cells.[43,44]

ROCK1 can also be constitutively activated by the proteolytic cleavage of its inhibitory carboxyl-terminal domain. ROCK1 is cleaved by caspase-3 at DETD1113 during apoptosis.[10,11] Caspase-3 is believed to be responsible for activating ROCK1 in apoptotic cells.[10–12,14] Our results strongly support the hypothesis that ROCK1 is activated by caspase-3, rather than RhoA, during triptolide-mediated apoptosis. Cotreating U937 and AML cells with triptolide and a caspase inhibitor (z-VAD-fmk or z-DEVD-fmk) significantly abrogated the ROCK1 activation induced by

triptolide (Figure 5c). Triptolide also did not induce RhoA activation (Figure 4a). In fact, pretreating cells with C3, a RhoA inhibitor, did not abrogate or attenuate triptolide-mediated ROCK1 activation, caspase-3, caspase-9, and PARP cleavage, or apoptosis (Figures 5d–f). Thus, caspase-3 is likely responsible for ROCK1 activation during triptolide-mediated apoptosis. Most interestingly, activation of ROCK1 mediated by triptolide also promoted caspase-3 activation and apoptosis. Inhibition of ROCK1 by Y-27632, a ROCK1 inhibitor, effectively blocked caspase-3 activation and apoptosis mediated by triptolide (Figures 7a and b). Furthermore, knocked down ROCK1 expression by a ROCK1-specific siRNA also prevented triptolide-induced caspase-3 activation and apoptosis (Figures 7d and e). Such findings suggest that activation of ROCK1 generated a positive feedback loop for caspase-3 activation.

ROCK1 activation results in the phosphorylation of various target proteins, including MLC[6] and MYPT.[7] Caspase-3-mediated ROCK1 activation is responsible for increased MLC phosphorylation in various cell types,[10,11] and increased MLC phosphorylation can stimulate actomyosin contractility.[45] Our results showed that triptolide increased both MLC and MYPT phosphorylation (Figure 4a), both of which were effectively blocked by Y-27632, a ROCK1 inhibitor (Figure 7c). Y-27632 also prevented triptolide-induced apoptosis (Figure 7a). RhoA inhibition by C3 did not prevent triptolide-induced MLC phosphorylation (Figure 5f); in contrast, the caspase inhibitors z-VAD-fmk and z-DEVD-fmk were able to abrogate the triptolide-induced MLC phosphorylation (Figure 5c). Furthermore, ML-7, a specific MLC inhibitor, significantly prevented
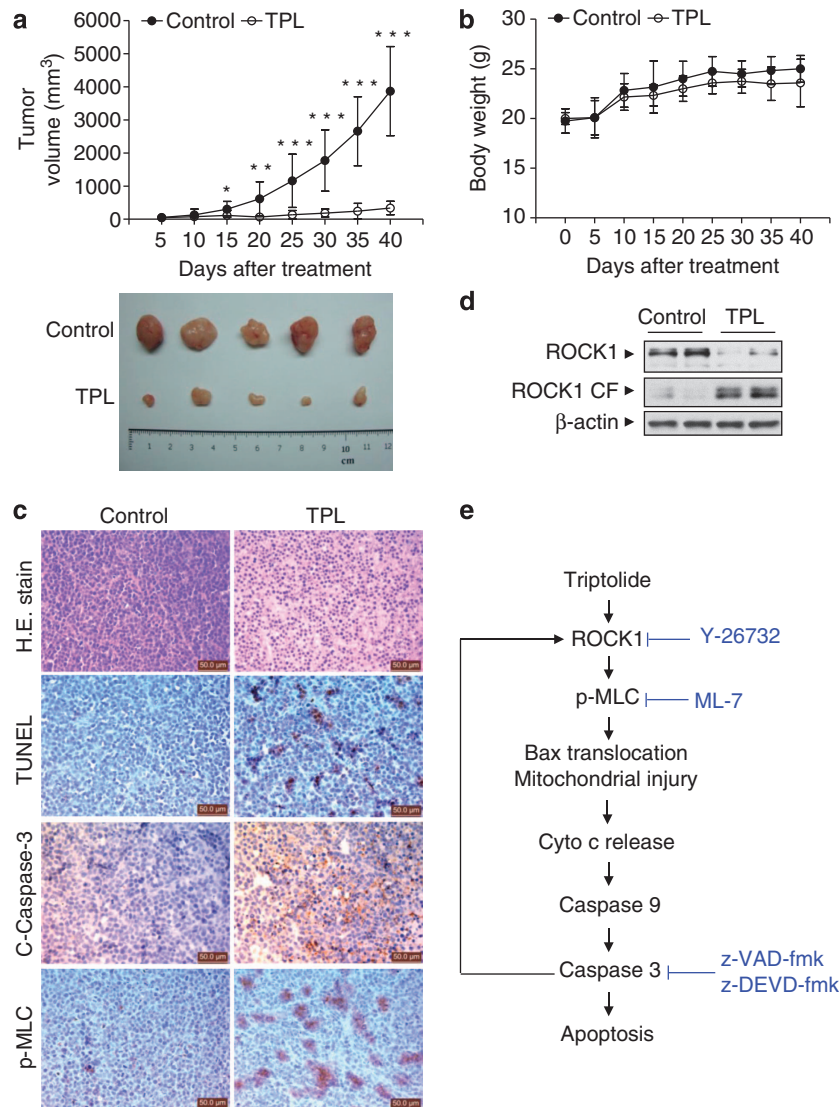
Figure 8 Triptolide inhibited the growth of U937 xenografts. A total of 24 nude mice were inoculated with U937 cells and randomly divided into two groups (12 mice/group) that were treated with either vehicle or triptolide. (**a**) Tumor volumes were measured at the indicated intervals (upper panel) and images are shown for five representative tumors from each group after 40 days of treatment (lower panel). Data are shown as the mean ± S.D. *$P<0.05$; **$P<0.01$; ***$P<0.001$. (**b**) Changes in body weight in the mice during 40 days of triptolide treatment. (**c**) Tumors were fixed and stained with H&E to examine tumor cell morphology. TUNEL assays were used to determine the apoptotic effects of triptolide. Immunohistochemistry was used to determine the levels of cleaved caspase-3 and phospho-MLC. Scale bar represents 50 μm. (**d**) After treatment, tumors from the vehicle and triptolide groups were lysed and subjected to immunoblotting with anti-ROCK1. Results are representative of three independent experiments. (**e**) An illustration of the molecular mechanism of triptolide-induced apoptosis. Exposure to triptolide results in activation of ROCK1 and MLC and MYPT phosphorylation, leading in turn to Bax translocation, culminating in cytochrome *c* release (Cyto *c*), caspases activation, and apoptosis. Activated caspase-3 in turn causes activation of ROCK, thus creating a positive feedback loop

the increase in apoptosis induced by triptolide (Figure 6a). Together, these findings further support the role of caspase-3, rather than RhoA, in activating ROCK1 during triptolide-mediated apoptosis. ROCK1 then phosphorylates MLC and MYPT that leads to apoptosis.

In summary, our present findings indicate that triptolide effectively induces apoptosis in human leukemia cells, including primary leukemia blasts, and inhibits the tumor growth of leukemia xenografts. These effects are associated with ROCK1 activation and MLC and MYPT phosphorylation. Our results also suggest that ROCK1 is cleaved by caspase-3, rather than RhoA, in this process. The activation of ROCK1

then further promotes caspase-3 activation and apoptosis induced by triptolide. The activation of ROCK1 and caspase-3 might represent a positive feedback loop resulting in triptolide-mediated apoptosis (Figure 8e). The ROCK1 activation and MLC phosphorylation mediated by triptolide could be a potential therapeutic intervention for treating leukemia and potentially other hematologic malignancies.

Materials and Methods

Reagents and compounds. Triptolide was purchased from Alexis Biochemicals (San Diego, CA, USA); z-Asp-Glu-Vad-Asp(Ome)-fluoromethylk-etone (z-DEVD-fmk) and z-Val-Ala-Asp(Ome)-fluoromethylketone (z-VAD-fmk)

from Enzyme Systems Products (Livermore, CA, USA); exoenzyme C3 and 1-(5-iodonapthalene-1-sulfonyl) homopiperazine hydrochloride (ML-7) from Calbiochem (La Jolla, CA, USA); and Y-27632 from Santa Cruz Biotechnology (Santa Cruz, CA, USA).

Antibodies against cleaved caspase-3, cleaved caspase-9, cytochrome c oxidase (COX)-IV, RhoA, MLC, phospho-MLC (Thr18/Ser19), MYPT1, and phospho-MYPT1 (Thr696) were purchased from Cell Signaling Technology (Beverly, MA, USA). Antibodies against AIF, cytochrome c, β-actin, and histone H1 were purchased from Santa Cruz Biotechnology. Antibodies against PARP, Bax, and ROCK1 were purchased from Epitomics (Burlingame, CA, USA). Alexa Fluor 647 donkey anti-rabbit IgG and Alexa Fluor 488 donkey anti-rabbit IgG were purchased from Invitrogen (Grand Island, NY, USA).

Cell isolation and culture. Human leukemia cell lines U937, Jurkat and HL-60 were purchased from American Type Culture Collection (ATCC, Manassas, VA, USA). Cells were cultured in RPMI-1640 medium supplemented with 10% fetal bovine serum (FBS) at 3.5×10^5/ml. Fresh primary leukemia patient samples and normal bone marrow specimens were acquired after obtaining informed consent, according to institutional guidelines and the declaration of Helsinki. Approval was obtained from the Southwest Hospital (Chongqing, China) Institutional Review Board for these studies. Mononuclear cells were isolated from the samples using Ficoll-Plaque (Pharmacia Biotech, Piscataway, NY, USA) density gradient separation. Cells were suspended at 1×10^6/ml and cultured in RPMI-1640 medium supplemented with 10% FBS.

Apoptosis assay. Apoptotic cells were identified by FITC-conjugated Annexin V/propidium iodide (PI) staining (BD Pharmingen, San Diego, CA, USA) according to the manufacturer's instructions, and analyzed with a FACSCalibur flow cytometer (Becton Dickinson, San Jose, CA, USA). Both early apoptotic (Annexin V-positive, PI-negative) and late apoptotic (Annexin V-positive and PI-positive) cells were included in cell death measures.

To determine levels of apoptosis in normal CD34$^+$ cells, cells were incubated with anti-CD34-phycoerythrin (anti-CD34-PE; Becton Dickinson, for 20 min. FITC-conjugated Annexin V/PI staining was then used. The proportion of cells undergoing treatment that were apoptotic was calculated according to apoptosis levels observed in the normal CD34$^+$ cells.

Mitochondrial membrane potential (MMP). After triptolide treatment, U937 cells were collected and washed twice in 0.1 M phosphate-buffered saline (PBS). Cells were then resuspended in PBS at 1×10^5/ml, and rhodamine-123 (Sigma-Aldrich, Saint-Louis, MO, USA) at a final concentration of $1 \mu M$ was added. After incubating for 30 min at 37 °C, cells were washed twice with PBS and then analyzed using FACSCalibur flow cytometer at an excitation wavelength of 488 nm and an emission wavelength of 525 nm. Fluorescent signal intensity was examined by Cellguest software (Becton Dickinson). For each sample, 10 000 events were collected, and MMP was assessed by mean fluorescence intensity.

Immunoblotting. Immunoblotting analysis was performed as described previously.[46] Briefly, treated cells were washed with PBS and lysed in $1 \times$ NuPAGE LDS sample buffer (Invitrogen, Carlsbad, CA, USA) to obtain total protein lysates. Mitochondrial and cytosolic fractions were obtained using the Cell Mitochondria Isolation Kit (Beyotime, Jiangsu, China), and nuclear extracts were obtained using the Nuclear and Cytoplasmic Protein Extraction Kit (Beyotime). Protein concentrations were determined using the Enhanced BCA Protein Assay Reagent (Beyotime). Equal amounts of cell lysate were loaded onto SDS-PAGE gels and then transferred to PVDF membranes. Membranes were blocked with 5% fat-free dry milk in Tris-buffered saline (TBS), containing 0.05% Tween-20, and incubated with primary antibodies. Protein bands were detected by horseradish peroxidase-conjugated species-specific secondary antibodies (Kirkegaard and Perry Laboratories, Gaithersburg, MD, USA). Bands were visualized with enhanced chemiluminescence reagent (Perkin-Elmer Life Sciences, Boston, MA, USA).

Immunofluorescence. Immunofluorescence analysis was performed as described previously.[47] Briefly, cells were fixed in 4% paraformaldehyde for 30 min and then permeabilized by 0.1% Triton X-100 in PBS for 15 min at room temperature. Next, cells were blocked with 3% bovine serum albumin in PBS for 30 min at room temperature. To detect nuclear accumulation of AIF, cells were further incubated with primary polyclonal anti-AIF antibody (1 : 50) at 4 °C overnight, followed by secondary Alexa Fluor 647 donkey anti-rabbit IgG (1 : 300)

for 1 h at room temperature. After washing, nuclei were counterstained for 10 min with 0.1 mg/ml 4′, 6-diamidino-2-phenylindole (DAPI; Sigma-Aldrich) and then sealed in anti-fade reagent (Beyotime).

To analyze Bax and mitochondrial colocalization, cells were pretreated with 500 nM MitoTracker Red CMXRos (Invitrogen-Molecular Probes, Eugene, OR, USA) for 30 min at 37 °C, washed three times in PBS, and then treated with triptolide. After treatment, cells were fixed and blocked. Next, cells were incubated with primary polyclonal anti-Bax antibody (1 : 50) at 4 °C overnight, followed by secondary Alexa Fluor 488 donkey anti-rabbit IgG (1 : 300) for 1 h at room temperature. After washing in PBS, the slides were sealed with anti-fade reagent. Confocal micrographs were taken by a laser confocal scanning microscope (TCS SP5; Leica Microsystems, Mannhein, Germany).

RhoA activation assay. RhoA-GTP levels were assessed with Rhotekin Rho Binding Domain-GST-Fusion, Human, Recombinant, Agarose Conjugate (Calbiochem, San Diego, CA, USA) according to the manufacturer's recommendations. Briefly, cells were rapidly lysed at 4 °C and incubated with Rhotekin-RBD affinity beads to specifically pull down RhoA-GTP. Cells were then centrifuged at 2000 r.p.m. for 2 min and washed in Wash Buffer. RhoA levels were quantified by running bead/protein complexes in loading buffer containing 0.1 M DTT. Bound RhoA-GTP was detected by incubating with a RhoA-specific antibody, followed by a secondary horseradish peroxidase-conjugated antibody. Reactive proteins were visualized by enhanced chemiluminescence.

RNA interference. The siRNA-encoding sequences against ROCK1 (5′-CAGCAAAGAGAGTGATATTCTCGAGAATATCACTCTCTTTGCTG-3′) were constructed in lentiviral RNAi vectors (hU6-MCS-ubiquitin-EGFP-IRES-puromycin). Scrambled siRNA was used as a negative control. Lentiviral vectors were co-transfected into 293Ta cells, and the lentiviral supernatant was harvested 48 h after transfection. U937 cells were infected by lentiviral supernatant with 5 mg/ml polybrene; infected cells were then selected for by 5 mg/ml puromycin. Thereafter, cells from each clone were analyzed for ROCK1 expression by western blots, and the most efficient siRNA downregulating ROCK1 expression was used in all experiments.

Xenograft assay. Nude mice, aged 5 weeks, were purchased from Vital River Laboratories (VRL, Beijing, China). Animal studies were approved by the university institutional animal care and use committee. U937 cells (total: 2×10^6 cells) were resuspended in a 1 : 1 ratio (total volume: 100 μl) in serum-free RPMI-1640 medium with a Matrigel basement membrane matrix. U937 cells were injected subcutaneously into the right flanks of the mice. Mice were randomized into two groups ($n = 12$ for each group). At 5 days after tumor inoculation, mice received either triptolide (0.15 mg/kg, intraperitoneally for 40 days) or an equal volume of vehicle control. Tumor volume and body weight were measured every 5 days. Tumor volumes were determined by measuring tumor length (l) and width (w), and then calculating the tumor volume using $V = lw^2/2$. Mice were killed after 40 days of drug exposure, and tumor tissues were fixed in paraformaldehyde. Paraffin-embedded and sectioned tissues were processed for H&E staining. The TUNEL assay was performed according to the manufacturer's instructions using the In Situ Cell Death Detection kit (Roche, Mannheim, Germany) to detect apoptosis in the tumor tissues. Immunohistochemistry was performed as previously described.[48]

Statistical analyses. Results were expressed as mean ± S.D. of at least five independent experiments. Comparisons between groups were evaluated by Student's t-test. *$P < 0.05$, **$P < 0.01$, ***$P < 0.001$ were considered statistically significant.

Conflict of Interest

The authors declare no conflict of interest.

Author Contributions

LL, GL, QL, ZJ, LZ, JZ, XH, TZ, and JC performed experiments; LL and NG analyzed the results and prepared the figures; NG, LL, and JC designed the study and wrote the paper.

1. Etienne-Manneville S, Hall A. Rho GTPases in cell biology. *Nature* 2002; **420**: 629–635.
2. Matsui T, Amano M, Yamamoto T, Chihara K, Nakafuku M, Ito M *et al.* Rho-associated kinase, a novel serine/threonine kinase, as a putative target for small GTP binding protein Rho. *EMBO J* 1996; **15**: 2208–2216.
3. Amano M, Fukata Y, Kaibuchi K. Regulation and functions of Rho-associated kinase. *Exp Cell Res* 2000; **261**: 44–51.
4. Shi J, Wei L. Rho kinase in the regulation of cell death and survival. *Arch Immunol Ther Exp (Warsz)* 2007; **55**: 61–75.
5. Ishizaki T, Maekawa M, Fujisawa K, Okawa K, Iwamatsu A, Fujita A *et al.* The small GTP-binding protein Rho binds to and activates a 160kDa Ser/Thr protein kinase homologous to myotonic dystrophy kinase. *EMBO J* 1996; **15**: 1885–1893.
6. Kureishi Y, Kobayashi S, Amano M, Kimura K, Kanaide H, Nakano T *et al.* Rho-associated kinase directly induces smooth muscle contraction through myosin light chain phosphorylation. *J Biol Chem* 1997; **272**: 12257–12260.
7. Kimura K, Ito M, Amano M, Chihara K, Fukata Y, Nakafuku M *et al.* Regulation of myosin phosphatase by Rho and Rho-associated kinase (Rho-kinase). *Science* 1996; **273**: 245–248.
8. Amano M, Chihara K, Kimura K, Fukata Y, Nakamura N, Matsuura Y *et al.* Formation of actin stress fibers and focal adhesions enhanced by Rho-kinase. *Science* 1997; **275**: 1308–1311.
9. Leung T, Chen XQ, Manser E, Lim L. The p160 RhoA-binding kinase ROK alpha is a member of a kinase family and is involved in the reorganization of the cytoskeleton. *Mol Cell Biol* 1996; **16**: 5313–5327.
10. Coleman ML, Sahai EA, Yeo M, Bosch M, Dewar A, Olson MF. Membrane blebbing during apoptosis results from caspase-mediated activation of ROCK I. *Nat Cell Biol* 2001; **3**: 339–345.
11. Sebbagh M, Renvoize C, Hamelin J, Riche N, Bertoglio J, Breard J. Caspase-3-mediated cleavage of ROCK I induces MLC phosphorylation and apoptotic membrane blebbing. *Nat Cell Biol* 2001; **3**: 346–352.
12. Parent N, Sane AT, Droin N, Bertrand R. Procaspase-2S inhibits procaspase-3 processing and activation, preventing ROCK-1-mediated apoptotic blebbing and body formation in human B lymphoma Namalwa cells. *Apoptosis* 2005; **10**: 313–322.
13. Ueda H, Morishita R, Itoh H, Narumiya S, Mikoshiba K, Kato K *et al.* Galpha11 induces caspase-mediated proteolytic activation of Rho-associated kinase, ROCK-I, in HeLa cells. *J Biol Chem* 2001; **276**: 42527–42533.
14. Chang J, Xie M, Shah VR, Schneider MD, Entman ML, Wei L *et al.* Activation of Rho-associated coiled-coil protein kinase 1 (ROCK-1) by caspase-3 cleavage plays an essential role in cardiac myocyte apoptosis. *Proc Natl Acad Sci USA* 2006; **103**: 14495–14500.
15. Brinker AM, Ma J, Lipsky PE, Raskin I. Medicinal chemistry and pharmacology of genus Tripterygium (Celastraceae). *Phytochemistry* 2007; **68**: 732–766.
16. Liu Q. Triptolide and its expanding multiple pharmacological functions. *Int Immunopharmacol* 2011; **11**: 377–383.
17. Carter BZ, Mak DH, Schober WD, McQueen T, Harris D, Estrov Z *et al.* Triptolide induces caspase-dependent cell death mediated via the mitochondrial pathway in leukemic cells. *Blood* 2006; **108**: 630–637.
18. Mak DH, Schober WD, Chen W, Konopleva M, Cortes J, Kantarjian HM *et al.* Triptolide induces cell death independent of cellular responses to imatinib in blast crisis chronic myelogenous leukemia cells including quiescent CD34+ primitive progenitor cells. *Mol Cancer Ther* 2009; **8**: 2509–2516.
19. Lou YJ, Jin J. Triptolide down-regulates bcr-abl expression and induces apoptosis in chronic myelogenous leukemia cells. *Leuk Lymphoma* 2004; **45**: 373–376.
20. Carter BZ, Mak DH, Schober WD, Dietrich MF, Pinilla C, Vassilev LT *et al.* Triptolide sensitizes AML cells to TRAIL-induced apoptosis via decrease of XIAP and p53-mediated increase of DR5. *Blood* 2008; **111**: 3742–3750.
21. Liu J, Shen M, Yue Z, Yang Z, Wang M, Li C *et al.* Triptolide inhibits colon-rectal cancer cells proliferation by induction of G1 phase arrest through upregulation of p21. *Phytomedicine* 2012; **19**: 756–762.
22. Jiang XH, Wong BC, Lin MC, Zhu GH, Kung HF, Jiang SH *et al.* Functional p53 is required for triptolide-induced apoptosis and AP-1 and nuclear factor-kappaB activation in gastric cancer cells. *Oncogene* 2001; **20**: 8009–8018.
23. Westerheide SD, Kawahara TL, Orton K, Morimoto RI. Triptolide, an inhibitor of the human heat shock response that enhances stress-induced cell death. *J Biol Chem* 2006; **281**: 9616–9622.
24. Guo Q, Nan XX, Yang JR, Yi L, Liang BL, Wei YB *et al.* Triptolide inhibits the multidrug resistance in prostate cancer cells via the downregulation of MDR1 expression. *Neoplasma* 2013; **60**: 598–604.
25. Park SW, Kim YI. Triptolide induces apoptosis of PMA-treated THP-1 cells through activation of caspases, inhibition of NF-kappaB and activation of MAPKs. *Int J Oncol* 2013; **43**: 1169–1175.
26. Kim MJ, Lee TH, Kim SH, Choi YJ, Heo J, Kim YH. Triptolide inactivates Akt and induces caspase-dependent death in cervical cancer cells via the mitochondrial pathway. *Int J Oncol* 2010; **37**: 1177–1185.
27. Zhou GS, Hu Z, Fang HT, Zhang FX, Pan XF, Chen XQ *et al.* Biologic activity of triptolide in t(8;21) acute myeloid leukemia cells. *Leuk Res* 2011; **35**: 214–218.
28. Zhou ZL, Yang YX, Ding J, Li YC, Miao ZH. Triptolide: structural modifications, structure-activity relationships, bioactivities, clinical development and mechanisms. *Nat Prod Rep* 2012; **29**: 457–475.
29. Yang J, Liu X, Bhalla K, Kim CN, Ibrado AM, Cai J *et al.* Prevention of apoptosis by Bcl-2: release of cytochrome c from mitochondria blocked. *Science* 1997; **275**: 1129–1132.
30. Danial NN, Korsmeyer SJ. Cell death: critical control points. *Cell* 2004; **116**: 205–219.
31. Riento K, Ridley AJ. Rocks: multifunctional kinases in cell behaviour. *Nat Rev Mol Cell Biol* 2003; **4**: 446–456.
32. Feng J, Ito M, Ichikawa K, Isaka N, Nishikawa M, Hartshorne DJ *et al.* Inhibitory phosphorylation site for Rho-associated kinase on smooth muscle myosin phosphatase. *J Biol Chem* 1999; **274**: 37385–37390.
33. Kawano Y, Fukata Y, Oshiro N, Amano M, Nakamura T, Ito M *et al.* Phosphorylation of myosin-binding subunit (MBS) of myosin phosphatase by Rho-kinase in vivo. *J Cell Biol* 1999; **147**: 1023–1038.
34. Zhang Y, Gu X, Yuan X. Phenylalanine activates the mitochondria-mediated apoptosis through the RhoA/Rho-associated kinase pathway in cortical neurons. *Eur J Neurosci* 2007; **25**: 1341–1348.
35. Yang S, Chen J, Guo Z, Xu XM, Wang L, Pei XF *et al.* Triptolide inhibits the growth and metastasis of solid tumors. *Mol Cancer Ther* 2003; **2**: 65–72.
36. Wang X. The expanding role of mitochondria in apoptosis. *Genes Dev* 2001; **15**: 2922–2933.
37. Green DR, Kroemer G. The pathophysiology of mitochondrial cell death. *Science* 2004; **305**: 626–629.
38. Shamas-Din A, Kale J, Leber B, Andrews DW. Mechanisms of action of Bcl-2 family proteins. *Cold Spring Harb Perspect Biol* 2013; **5**: a008714.
39. Wu PP, Liu KC, Huang WW, Ma CY, Lin H, Yang JS *et al.* Triptolide induces apoptosis in human adrenal cancer NCI-H295 cells through a mitochondrial-dependent pathway. *Oncol Rep* 2011; **25**: 551–557.
40. Shi X, Jin Y, Cheng C, Zhang H, Zou W, Zheng Q *et al.* Triptolide inhibits Bcr-Abl transcription and induces apoptosis in STI571-resistant chronic myelogenous leukemia cells harboring T315I mutation. *Clin Cancer Res* 2009; **15**: 1686–1697.
41. Lochhead PA, Wickman G, Mezna M, Olson MF. Activating ROCK1 somatic mutations in human cancer. *Oncogene* 2010; **29**: 2591–2598.
42. Miñambres R, Guasch RM, Perez-Aragó A, Guerri C. The RhoA/ROCK-I/MLC pathway is involved in the ethanol-induced apoptosis by anoikis in astrocytes. *J Cell Sci* 2006; **119**: 271–282.
43. Feng J, Ito M, Kureishi Y, Ichikawa K, Amano M, Isaka N *et al.* Rho-associated kinase of chicken gizzard smooth muscle. *J Biol Chem* 1999; **274**: 3744–3752.
44. Morikage N, Kishi H, Sato M, Guo F, Shirao S, Yano T *et al.* Cholesterol primes vascular smooth muscle to induce Ca^{2+} sensitization mediated by a sphingosylphosphorylcholine-Rho-kinase pathway: possible role for membrane raft. *Circ Res* 2006; **99**: 299–306.
45. Mills JC, Stone NL, Erhardt J, Pittman RN. Apoptotic membrane blebbing is regulated by myosin light chain phosphorylation. *J Cell Biol* 1998; **140**: 627–636.
46. Zhou T, Li G, Cao B, Liu L, Cheng Q, Kong H *et al.* Downregulation of Mcl-1 through inhibition of translation contributes to benzyl isothiocyanate-induced cell cycle arrest and apoptosis in human leukemia cells. *Cell Death Dis* 2013; **4**: e515.
47. Li G, Cheng Q, Liu L, Zhou T, Shan CY, Hu XY *et al.* Mitochondrial translocation of cofilin is required for allyl isothiocyanate-mediated cell death via ROCK1/PTEN/PI3K signaling pathway. *Cell Commun Signal* 2013; **11**: 50.
48. Li G, Zhou T, Liu L, Chen J, Zhao Z, Peng Y *et al.* Ezrin dephosphorylation/downregulation contributes to ursolic acid-mediated cell death in human leukemia cells. *Blood Cancer J* 2013; **3**: e108.

Supplementary Information accompanies this paper on Cell Death and Disease website (http://www.nature.com/cddis)